IL NUOVO CIMENTO **45 C** (2022) 53
DOI 10.1393/ncc/i2022-22053-4

Colloquia: IWM-EC 2021

Study of the symmetry energy from ^{48,40}Ca+^{48,40}Ca collisions at 35 AMeV

Q. Fable(1)(2)(3) and A. Chbihi(2) for the INDRA Collaboration

(1) *Laboratoire des 2 Infinis, Toulouse (L2IT-IN2P3), Universitè de Toulouse, CNRS, UPS F-31062 Toulouse Cedex 9, France*
(2) *GANIL, CEA/DRF-CNRS/IN2P3 - Bvd. Henri Becquerel, F-14076 Caen Cedex, France*
(3) *Normandie Univ, ENSICAEN, UNICAEN, CNRS/IN2P3, LPC Caen - F-14000 Caen, France*

received 12 May 2022

Summary. — In this proceeding we present recent results concerning the study of the symmetry energy coefficient of finite nuclei with ^{40,48}Ca+^{40,48}Ca peripheral to semi-peripheral reactions at 35 MeV/nucleon. Data were obtained using the unique coupling of the VAMOS high acceptance spectrometer and the INDRA detector. VAMOS allowed high resolution measurement of charge, mass and velocity of the cold projectile-like fragment (PLF), while the INDRA detector recorded coincident charged particles with nearly 4π acceptance. This coupling allows reconstructing the mass, charge and excitation energy of the associated initial quasi-projectile nuclei (QP), as well as the extraction of apparent temperatures. The isoscaling method was applied with the fragment identified in VAMOS and the experimental reconstructed QP, in order to estimate the surface to volume contribution of the symmetry energy term of finite nuclei.

1. – Context and motivations

The Bethe-Weizsäcker semi-empirical mass formula allows describing the ground-state binding energy per nucleon of nuclei, such as

$$B(N,Z) = -c_V + c_S A^{-1/3} + C_{sym}(A)\left(\frac{N-Z}{A}\right)^2 + E_C + \dots, \tag{1}$$

where c_V and c_S correspond to the volume and surface energy of symmetric mater, E_C the Coulomb energy of a uniformly charged sphere while C_{sym} is the symmetry energy. The simplest droplet model consists of an extension of eq. (1) to include a surface

asymmetry [1] that is required to describe the energies of light asymmetric nuclei [2]. This leads to a mass-dependent symmetry energy coefficient such as

$$C_{sym}(A) = a_V - a_S A^{-1/3}, \tag{2}$$

where a_V and a_S are the volume and surface components of the symmetry energy.

Analyzing the measured binding energies, a correlation was established between the volume and surface components [2]. The experimental information about the surface term is fairly limited while comparable results were obtained for the volume term; experimental data from the excitation energies of isobaric analog states lead for example to $15 \leq C_{sym} \leq 22\,\mathrm{MeV}$ and $30 \leq a_V \leq 34\,\mathrm{MeV}$ over the $30 \leq A \leq 240$ mass region [3].

2. – Experimental setup

The INDRA-VAMOS coupling was used at the GANIL facility to measure ^{48,40}Ca+^{48,40}Ca collisions at 35 MeV/nucleon.

The VAMOS high acceptance spectrometer [4] covered the forward polar angles from 2.56° to 6.50°, so as to detect a single fragment emitted slightly above the grazing angle of the collisions. Its detection chamber was composed of a 7-module ionization chamber, a 500 μm thick Si-wall (18 independent modules) and a 1 cm thick CsI(Tl)-wall (80 independent modules), allowing the measurements of the time of flight, energy loss and energy parameters. Two position-sensitive drift chambers were used to determine the trajectories of the reaction products at the focal plane. Around twelve magnetic rigidity ($B\rho_0$) settings, from 0.661 to 2.220 Tm, were measured for each system to cover the full velocity range of the fragments and identify isotopically the forward-emitted PLF.

INDRA [5] covered polar angles from 7° to 176° with detection telescopes arranged in rings centered around the beam axis. The forward rings (7°–45°) consisted each of three-layer detection telescopes: a gas-ionization chamber, a 300 or 150 μm silicon wafer and a CsI(Tl) scintillator (14 to 10 cm thick) read by a photomultiplier tube. The backward rings (45°–176°) included two-layer telescopes: a gas-ionization chamber and a CsI(Tl) scintillator (5 to 8 cm thick). INDRA allowed charge and isotope identification up to Be-B and only charge identification for heavier fragments.

The trigger condition of the experiment was a single hit on the VAMOS silicon wall in order to enhance the detection of peripheral collisions. Further details of the setup, trajectory reconstruction and normalization procedure can be found in [6, 7].

Figure 1 presents the chart of the nuclides identified in VAMOS for the ^{48}Ca+^{48}Ca reaction. We observe that a variety of neutron-rich isotopes are measured, showing the excellent isotopic identification obtained with VAMOS. Furthermore, the fragments measured in VAMOS are mostly in a region of charge and velocity close to the projectile ($10 < Z < 20$ and $6 < V_z < 8$ cm/ns), corresponding to a region associated with the PLF.

3. – Reconstruction method

Such coupling allows reconstructing the hot QP source from the remnant identified with VAMOS (assumed to be the PLF) and carefully selected LCP measured in INDRA. To isolate QP emissions, we applied a selection based on the relative velocities between the reaction products detected in INDRA and i) the PLF detected in VAMOS ($V_{rel,PLF}$),

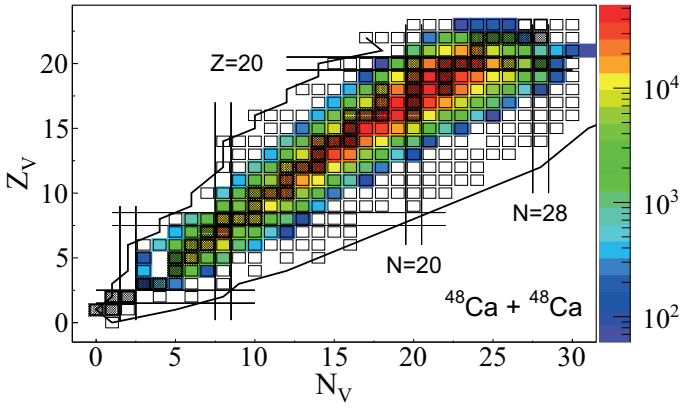

Fig. 1. – (Color online). Chart of nuclides identified in VAMOS for the ^{48}Ca+^{48}Ca reaction. Proton and neutron drip-lines are represented by solid lines, stable isotopes with blurred boxes.

ii) the fragment with the largest identified Z at backward angles in INDRA, supposed to be the TLF ($V_{rel,TLF}$). Numerically, only fragments verifying $\frac{V_{rel,TLF}}{V_{rel,PLF}} > 1.35$ for $Z = 1$ and $\frac{V_{rel,TLF}}{V_{rel,PLF}} > 1.75$ for $Z \geq 2$ were selected. More details about the reconstruction method can be found in [7].

Figure 2 shows the effect of the selection on the invariant cross section contours in the parallel *vs.* longitudinal velocity plots ($V_{\parallel} - V_{\perp}$ in the VAMOS fragment reference frame), for proton and α particles and two different isotopes in VAMOS. We observe that the

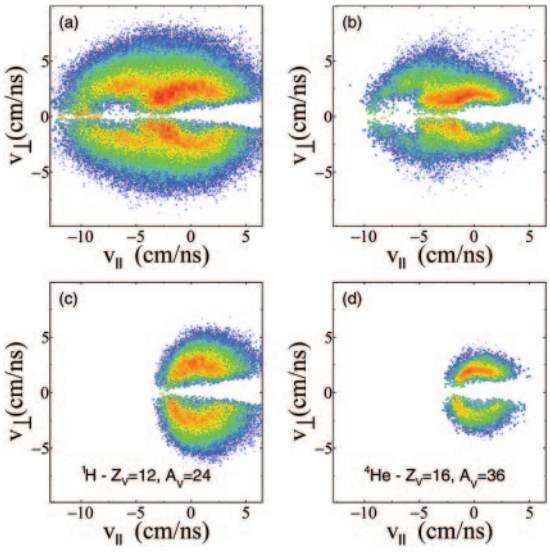

Fig. 2. – (Color online). Invariant cross section contours in the parallel *vs.* longitudinal velocity plots in the VAMOS fragment reference frame. (a) and (c): proton contours associated with a ^{24}Mg isotope in VAMOS with ^{40}Ca+^{40}Ca reaction, respectively before and after the selection. (b) and (d): α-particle contours associated with a ^{36}S isotope in VAMOS with ^{48}Ca+^{48}Ca reaction, respectively before and after the selection.

selection allows excluding the LCP originating from the QT source (components centered at $V_{\parallel} \simeq -8\,\mathrm{cm/ns}$) while the QP emissions are kept (components centered at $V_{\parallel} = 0$).

Using this previous selection, we can reconstruct the QP by summing the charges and masses of the fragment identified in VAMOS with the selected LCP and IMF isotopically identified with INDRA, on an event-by-event basis.

As the neutrons were not measured, the distributions of the neutrons evaporated by the reconstructed QP from filtered model calculations were employed as a substitute. The microscopic transport model AMD [8] was used to describe the dynamical evolution of the collisions. The AMD primary events produced at 300 *fm/c* were used as input for the evaporation model GEMINI++ [9,10]. Simulated events were filtered with a software replica of the experimental setup within the Kaliveda HIC analysis toolkit [11]. Finally, the same offline conditions as the experiment were applied to the filtered events.

The reconstructed QP charge Z_{QP} and the mass without neutrons $\widetilde{A}_{QP}$ were used to compute the neutron multiplicity, from a random number generator following the filtered model neutron distribution associated with the $(Z_{QP}, \widetilde{A}_{QP})$ combination, such as

$$A_{QP} = \widetilde{A}_{QP} + M_n^{rdm}(Z_{QP}, \widetilde{A}_{QP}), \tag{3}$$

where $M_n^{rdm}(Z_{QP}, \widetilde{A}_{QP})$ is the neutron multiplicity obtained from the random number generator.

4. – Symmetry energy coefficient estimation

4˙1. *Isoscaling.* – Information on the symmetry energy coefficient of finite nuclei C_{sym} can be inferred from the scaling behaviour, also called isoscaling, obtained from the ratio $R_{21}(N, Z)$ of the yields of the same isotope measured with two systems, $Y_{(1)}(N, Z)$ and $Y_{(2)}(N, Z)$, where (2) usually stands for the neutron-rich system [12]. Indeed, in a variety of HIC, an exponential dependence of the ratio on N and Z has been observed, such as

$$R_{21}(N, Z) = \frac{Y_{(2)}(N, Z)}{Y_{(1)}(N, Z)} \propto \exp\left[\alpha N + \beta Z\right], \tag{4}$$

where α and β are called the isoscaling parameters.

Assuming that the fragmenting sources can be described in the approximation of a grand canonical statistical ensemble, α and β can be expressed as $\alpha = \Delta\mu_n/T$ and $\beta = \Delta\mu_p/T$, where $\Delta\mu_n$ and $\Delta\mu_p$ are the differences between the neutron and proton chemical potentials and T the temperature of the decaying systems [13].

A Gaussian approximation of the yields in the grand-canonical approximation allows linking, for a given fragment charge Z, the α parameter to C_{sym}/T, such as [13-15]

$$\frac{4C_{sym}}{T} = \frac{\alpha}{(\frac{Z}{\langle A_1(Z)\rangle})^2 - (\frac{Z}{\langle A_2(Z)\rangle})^2}, \tag{5}$$

where $\langle A_1\rangle$ and $\langle A_2\rangle$ are the mean masses associated with the isotope charge Z for each system.

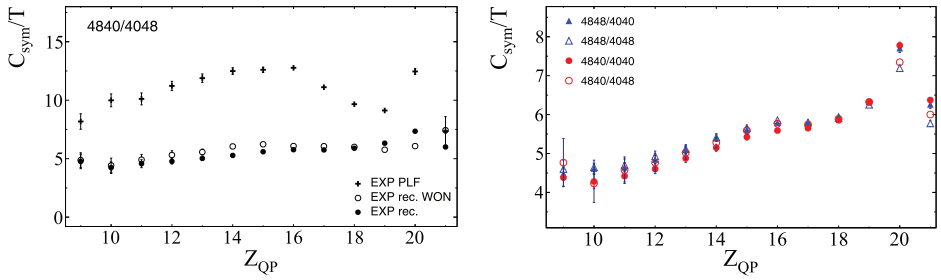

Fig. 3. – (Color online). (a) Comparison of the C_{sym}/T extracted from the isoscaling fits with the ^{48}Ca+^{40}Ca and ^{40}Ca+^{48}Ca combination, for the fragment identified in VAMOS (EXP PLF), the reconstructed QP without (EXP rec. WON) and with (EXP rec.) the evaporated neutron contribution. (b) C_{sym}/T extracted from the isoscaling fits for the reconstructed QP with the evaporated neutron contribution, for all combinations under study.

4˙2. *Isoscaling coefficients*. – Examples of the experimental isoscaling fits for the PLF and the reconstructed QP can be found in [7]. Using the α parameters extracted from isoscaling and the difference in average neutron composition of the two sources $\Delta = (Z/\langle A_1\rangle)^2 - (Z/\langle A_2\rangle)^2$, we study the behaviour of C_{sym}/T (see eq. (5)). An example is presented in fig. 3(a), with the ^{48}Ca+^{40}Ca and ^{40}Ca+^{48}Ca as the neutron-rich and neutron-deficient systems. Similar results are obtained with the other combinations under study. We observe higher values with a different trend for the PLF, compared to the QP. Concerning the reconstructed QP, an increase of C_{sym}/T is observed with increasing charge, independently of the free neutron contribution. This could be interpreted as a strong surface dependence of the symmetry energy term [15].

The rest of the analysis is focused only on the study of the isoscaling of the QP with the evaporated neutrons contribution. The corresponding C_{sym}/T are presented in fig. 3(b) for all system combinations under study. We observe remarkably close values for all combinations, increasing as a function of the size of the QP.

4˙3. *Apparent temperatures*. – The experimental apparent temperatures of the QP sources were extracted from the LCP measured in INDRA. We focused on the temperatures extracted from the slopes of the proton kinetic energy spectra in the reconstructed QP frame. The "3D Calorimetry" method was applied in order to only keep the LCP emitted in the forward domain of the reaction plane, where the QP acts as a screen to other emission sources, reducing the contamination from particles at high energy in the QP frame [16]. The apparent temperatures were then extracted by fitting the slope of the proton kinetic energy spectra in the forward domains with a Maxwell-Boltzmann distribution [17, 18].

The resulting apparent temperatures are presented in fig. 4. We observe a matching of the distributions according to the neutron-richness of the projectile, with relatively stable temperature around 3.75 MeV for the n-rich ^{48}Ca projectile reactions, while temperature increases from 3.25 to 3.5 MeV with decreasing Z_{QP} for the ^{40}Ca projectile reactions. Such pairing could be explained by the difference in grazing angle for the ^{40}Ca and ^{48}Ca projectile reaction, respectively $\theta^{40}_{gr} \simeq 2.3°$ and $\theta^{48}_{gr} \simeq 1.9°$. The drop in temperature observed for $Z_{QP} < 13$ with the ^{48}Ca+^{40}Ca collisions can be explained by a missing magnetic rigidity setting measurement for this system ($B\rho_0 = 0.782$ T·m).

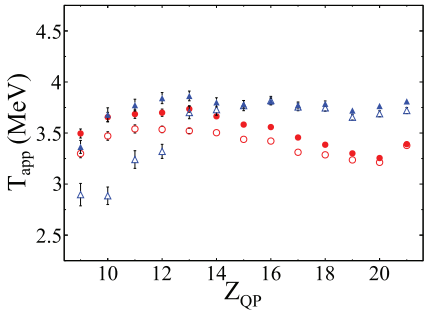

Fig. 4. – (Color online). Apparent temperatures as a function of the QP charge, extracted from proton kinetic energy spectra (see text). Same legend as fig. 3.

4˙4. *Symmetry energy coefficient estimation.* – Using the apparent temperatures presented in fig. 4 as the QP source temperatures, we estimate the symmetry coefficient from the isoscaling fits. The results are presented in fig. 5 as a function of the fragment charge. The average temperatures of the two systems at stake were used for the plots, while the temperatures of the ^{48}Ca+^{48}Ca system were used as a substitute for the ^{48}Ca+^{40}Ca in the $Z_{QP} < 13$ domain (in order to correct the missing magnetic rigidity setting). We observe that the estimated symmetry energy C_{sym} increases between 14 and 23 MeV with increasing charge of the QP. The overall values in the limited range of QP charge where the isoscaling is verified ($10 < Z_{QP} < 19$) are comparable with that of the bulk nuclear matter $C_{sym}(\rho_0)$ around $Z_{QP} \simeq 20$. A fit to the data (dashed line) leads to a surface-to-volume ratio $k = -a_S/a_V = 1.74 \pm 0.07$, with $a_V = 45.58 \pm 0.84$ and $a_S = -79.33 \pm 2.67$. Thus, the drop in temperature with increasing charge is not sufficient to explain the change in C_{sym}, which could be interpreted as a strong surface dependence [15]. In the opposite of [19], the observed Z-dependence of C_{sym} cannot be explained by a surface-to-volume ratio $k = 1.14$ for the symmetry energy of ground state nuclei in AMD (solid line). It should be noted that the estimated volume coefficient a_V remains high compared to the existing experimental data ($30 \leq a_V \leq 34$ MeV). Assum-

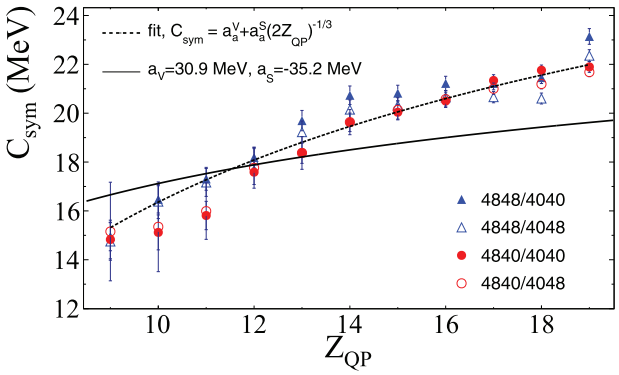

Fig. 5. – (Color online). Estimated symmetry energy coefficient C_{sym} from the isoscaling method, as a function of the charge of the reconstructed QP. The dashed line shows the fit of eq. (2) to the data with a reduced chi-square value $\chi^2 = 2.2$. The solid line shows the symmetry energy for the ground state nuclei in AMD ($a_V = 30.9$ MeV, $a_S = -35.2$ MeV [19]).

ing the temperatures are correct, this can be explained by the limited range of charges used in the present study ($9 \leq Z_{QP} \leq 19$).

5. – Conclusion

In this work, we presented a study of the symmetry energy coefficient of finite nuclei, based on the isoscaling method applied to peripheral to semi-peripheral ^{40,48}Ca+^{40,48}Ca collisions at 35 MeV/nucleon measured with the INDRA-VAMOS coupling at GANIL. A reconstruction method of the primary fragment was applied, by associating event-by-event the fragment identified with VAMOS (PLF) to the identified and selected particles detected with INDRA. The extracted C_{sym}/T as a function of the fragment charge exhibit a significant modification caused by the secondary decays, indicating that the reconstruction of the primary fragment is mandatory for the study of the symmetry energy coefficient at chemical freeze-out with such reactions. Concerning the reconstructed QP, increasing C_{sym}/T values with increasing charge are observed, in agreement with existing results obtained with isoscaling [20,21]. Applying the "3D Calorimetry" method, the apparent temperatures were extracted from the slope of the proton kinetic energy spectra, leading to relatively stable values around 3.6 MeV for all systems. The overall values of symmetry energy term are between 14 and 23 MeV, in the limited range of QP size (charge) where the isoscaling is verified. An increase in C_{sym} is also observed with increasing QP charge, which can be related to an effect of the surface contributions to the symmetry energy term, with a surface-to-volume ratio of $k = -a_S/a_V = 1.74 \pm 0.07$.

REFERENCES

[1] Myers W. D. and Swiatecki W. J., *Nucl. Phys.*, **81** (1966) 1.
[2] Danielewicz P., *Nucl. Phys. A*, **727** (2003) 233.
[3] Danielewicz P. and Lee J., *Nucl. Phys. A*, **922** (2014) 1.
[4] Pullanhiotan S., Rejmund M., Navin A., Mittig W. and Bhattacharyya S., *Nucl. Instrum. Methods Phys. Res. A*, **593** (2008) 343.
[5] INDRA Collaboration (Pouthas J. *et al.*), *Nucl. Instrum. Methods Phys. Res. A*, **357** (1995) 418.
[6] Fable Q., *Study of the isospin in ^{40,48}Ca+^{40,48}Ca collisions at 35 AMeV*, PhD Thesis, Normandie Université, 2018NORMC202 (2018).
[7] INDRA Collaboration (Fable Q. *et al.*), *Experimental study of the ^{40,48}Ca+ ^{40,48}Ca reactions at 35 MeV/nucleon*, arXiv:2202.13850 (2022).
[8] Akira Ono and Hisashi Horiuchi, *Prog. Part. Nucl. Phys.*, **53** (2004) 501.
[9] Charity R. J., *Phys. Rev. C*, **58** (1998) 1073.
[10] Charity R. J., Sobotka L. G. and Dickhoff W. H., *Phys. Rev. Lett.*, **97** (2006) 162503.
[11] *KaliVeda heavy-ion analysis toolkit; Toolkit for analysis & simulation of Fermi energy heavy-ion collisions*, `http://indra.in2p3.fr/kaliveda`.
[12] Tsang M. B. *et al.*, *Phys. Rev. Lett.*, **86** (2001) 5023.
[13] Ono A. *et al.*, *Phys. Rev. C*, **68** (2003) 051601.
[14] Raduta Ad. R. and Gulminelli F., *Phys. Rev. C*, **75** (2007) 044605.
[15] Raduta Ad. R. and Gulminelli F., *Phys. Rev. C*, **75** (2007) 024605.
[16] Vient E. *et al.*, *Phys. Rev. C*, **98** (2018) 044611.
[17] Weisskopf V., *Phys. Rev.*, **52** (1937) 295.
[18] Borderie B. and Frankland J. D., *Prog. Part. Nucl. Phys.*, **105** (2019) 82.
[19] Ono A. *et al.*, *Phys. Rev. C*, **70** (2004) 041604.
[20] Le Fèvre A. *et al.*, *Phys. Rev. Lett.*, **94** (2005) 162701.
[21] Souliotis G. A. *et al.*, *Phys. Rev. C*, **75** (2007) 011601.